Smart Structures and Systems, *Vol. 16, No. 1 (2015) 67-79*
DOI: http://dx.doi.org/10.12989/sss.2015.16.1.067

Experimental study on acoustic emission characteristics of reinforced concrete components

Aijun Gu[1, 2, 3], Ying Luo*[1,2] and Baiqiang Xu[4]

[1]*Key Laboratory for Mechanical Structure Damage Detection Technology, P.O. Box 84, Jiangsu University, Zhenjiang, China*
[2]*Faculty of Civil Engineering and Mechanics, Jiangsu University, Zhenjiang, China*
[3]*School of Hydraulic, Energy and Power Engineering, Yangzhou University, Yangzhou, China*
[4]*Faculty of Science, Jiangsu University, Zhenjiang, China*

(Received April 18, 2014, Revised August 24, 2014, Accepted August 26, 2014)

Abstract. Acoustic emission analysis is an effective technique for monitoring the evolution of damage in a structure. An experimental analysis on a set of reinforced concrete beams under flexural loading was carried out. A mixed AE analysis method which used both parameter-based and signal-based techniques was presented to characterize and identify different failure mechanisms of damage, where the signal-based analysis was performed by using the Hilbert-Huang transform. The maximum instantaneous energy of typical damage events and the corresponding frequency characteristics were established, which provided a quantitative assessment of reinforced concrete beam using AE technique. In the bending tests, a "pitch-catch" system was mounted on a steel bar to assess bonding state of the steel bar in concrete. To better understand the AE behavior of bond-slip damage between steel bar and concrete, a special bond-slip test called pullout test was also performed. The results provided the basis of quantitative AE to identify both failure mechanisms and level of damages of civil engineering structures.

Keywords: acoustic emission; reinforced concrete beam; four-point bending; Hilbert-Huang transform; bond-slip damage

1. Introduction

Acoustic emission (AE) is a transient wave resulting from the sudden release of stored energy during a damage process (Beattie 1983). It can be used to identify the evolution of damage in structures as a powerful nondestructive testing method while in service. In civil engineering, the complexity of material and different forms of components make the received AE signals very intricate, which have been challenging in damage identification. In earlier research, the AE parameters were recorded and analyzed to identify damages, which is known as the parameter-based (classical) method (Sagar and Prasad 2012). With advanced in computing power, the waveform of AE signals was analyzed as a diagnostic tool which was called signal-based method. Both methods are applied nowadays with some success for diverse applications. The parameter-based method is widely used in the actual project because of its high recording speed

*Corresponding author, Professor, E-mail: luoying@mail.ujs.edu.cn

http://www.techno-press.org/?journal=sss&subpage=8 ISSN: 1738-1584 (Print), 1738-1991 (Online)

and low requirement of equipment needed. However, due to the complication of materials in civil engineering, this method can be a significant limitation, and sometimes the conclusions can be misleading. On the other hand, a waveform carries all the information of AE from damages. Some authors began in the late 1980’s and in the early 1990’s with the theoretical development of quantitative techniques based on waveform analysis (Sachse and Kim 1987, Ono 1994). It has shown great potential in using AE technique for damage identification. Thus current trends definitely favor the signal-based techniques rather than others (Govekar *et al.* 2000, Grosse and Linzer 2008).

In AE technique, characterizing the AE sources is most critical. In signal-based method, the feature information which can effectively reflect the damage state of structures are extracted from AE waveform. Balázs *et al*. (1993) used coherence functions to assess the similarity of two different AE signals. Such an assessment is beneficial because the similar frequency content indicates the same source mechanism. But the method was under the premise that the influence of the medium and transducer characteristics could be ignored. Enoki and Kischi (1988) introduced a quantitative seismology theory into AE technique, and used an inversion method to determine the source mechanism in reinforced concrete (RC) beam. Yuyama *et al*. (1995), Ohtsu *et al*. (1998), and Grosse *et al.* (Grosse and Finck 2006) combined a moment tensor inversion (MTI) algorithm with a three-dimensional source localization to determine the fault plane solution that enables the analysis of the fracture process in the material. MTI is an inversion method which is used to determine the fracture type and orientation of a rupture (fault), as well as the seismic moment. In MTI (Yuyama *et al*. 1995, Ohtsu *et al.* 1998, Grosse and Finck 2006), a source of AE can be considered from a point source when the dominant wavelengths are much greater than the size of the damage, except the cases where multiple source emissions occur such as bond-slip. Further, the relationship between receiving signal and point source is represented by Green's function, which is rather difficult to determine in heterogeneous concrete materials, especially in actual civil structures containing reinforcement. The spectral analysis were also used in AE technique to describe the frequency feature of signals. But it is not suited to the case when the signal frequency characteristics are varying with time. A more reasonable method is time–frequency analysis. It comprises those techniques that study a signal in both the time and frequency domains simultaneously, using various time–frequency representations, such as short-time Fourier transform (STFT), wavelet analysis (Yoon *et al.* 2000), Hilbert-Huang transform (HHT) (Lu *et al*. 2011), and so on.

In comparison with the Fourier transform, wavelet transform is complete, orthogonal, local and adaptive, which are vital for forming a basis to analyze nonlinear and non-stationary signals. Hence, it can extract both the time and frequency features of the sensing signal effectively. However, wavelet methods may also prove to be inadequate because it is essentially an adjustable window Fourier spectral analysis and, although wavelet is well suited for analyzing data with gradual frequency changes, its non-locally adaptive approach causes leakage to bring spread frequency energy over a wider range (Lin and Chu 2012). HHT is a novel analysis method for nonlinear and non-stationary data, which was developed by Huang *et al*. (Huang and Shen 2005). HHT uses the apparent time scales revealed by the signal’s local maxima and minima to sequentially sift components of different time scales, starting from high-to low-frequency ones. Because HHT does not use pre-determined basis functions and function orthogonality for component extraction, it provides accurate instantaneous amplitudes and frequencies of extracted components for accurate estimation of system characteristics and nonlinearities (Frank Pai and Palazotto 2008). In addition, HHT does not involve any convolution, and the time used for computation is less and deemed suitable for analyzing signals. HHT has been applied in the field of AE research in recent years. Lin *et al*. (Lin and Chu 2012) applied HHT method on AE feature extraction of natural fatigue cracks in rotating shafts. Law *et al*. (2012) studied the spindle bearings condition monitoring used AE technique. The HHT analysis was used to extract the crucial characteristic from the measured data to correlate spindle running condition. Han *et al*. (Han and Zhou 2013) used HHT method to identify characteristic signal features associated with damage propagation for each failure mode in a carbon-fiber-reinforced twill-weave laminate under tensile loading. Hamdi *et al*. (2013) used HHT to study AE signals collected from unidirectional glass-fiber reinforced polymer composites samples. However, very little research on concrete components using HHT has been reported.

Though the reliability of the data interpretation can be improved significantly by using signal-based method, there are some inherent drawbacks in this technique. First, a large number of signals have to be stored digitally in data acquisition. Not all the events are recorded in waveform because of the limitation of AE system. Second, the signal-based analyzing process is time-consuming, and is hardly applied to each AE event. In addition, due to the influence of specimen geometry, material property, orientation of sensors, sensor capability, and performance of equipment, signals from different sensors always show different features.

The parameter-based method has been also developed in recent years. Some new parameters which gave more reasonable expression of AE characteristics were presented to identify AE source effectively (Aggelis *et al.* 2013, Aldahdooh and Bunnori 2013). But these parameters reflecting global property of signals and ignoring local features cannot satisfy the source identification in civil engineering.

More researchers trended to combine the parameter-based and signal-based techniques to leverage strengths. Yoon *et al*. (2000) used both parameter-based and signal-based AE technique to characterize and identify different sources of damage including microcrack development, localized crack propagation, and debonding of the reinforcing steel. It was verified that different failure mechanisms exhibit different AE characteristics. The waveform analysis was conducted using both fast Fourier transform and wavelet transform methods. Lin *et al*. (Lin and Chu 2011) applied AE technique on monitoring an offshore structure model. By using HHT method, the instantaneous frequency and energy information were extracted, which gave sharp identification of fundamental properties of crack AE signals. The conventional parameter-based AE analysis was also provided for comparison. However, the studies seems to focus more on the comparison of two methods than on complementary advantage.

In this study, the AE behavior of RC beams was investigated to characterize and identify different sources of damage. A notched short beam embedded a steel bar was designed under flexural loading to carry out a complex damage state. A “pitch-catch” device was used at steel bar to help identifying bonding state of steel bar in RC beam. A mixed method which used both parameter-based and signal-based method was presented in AE analysis. The AE signal characteristics were extracted by means of HHT which was verified as an effective method for nonlinear and non-stationary signals. The maximum instantaneous energy and the corresponding instantaneous frequency of typical signals were presented which gave both mechanism and level of the damages. These would provide a quantitative assessment to RC beam in AE technique.

2. Experiments

2.1 Bending test of RC beam

The RC beam was 100 mm wide, 150 mm high, and 600 mm long as shown in Fig. 1(a). A steel bar with diameter of 10 mm was embedded in the tensile zone of the beam. A notch was preset also in the tensile side of the beam to induce cracking. Four wide-band AE sensors (PAC WDI-AST) were attached to the surface of the beam by couplant to collect AE signals. The tests were performed on a MTS system. The experimental setup was shown in Fig. 1(b). The displacement controlled loading method was used with the loading velocity of 2 mm/min.

The bending test of the RC beam primarily introduces fracture damage. While in the later stage, the bond-slip may emerge at the interface between steel bar and concrete. Therefore, the identification of damage state during bending test is necessary in AE characteristic study.

The use of strain gauges at selected locations embedded in reinforcement and concrete is an effective means to detect any bond slip, and has been widely used by other researchers. However, the method has a distinct disadvantage, i.e., the strain gauges and their protection would change the slipping feature, and consequently, influence the AE signal characteristics. To overcome this disadvantage, apart from previous traditional methods, an active detecting method to monitor the slippage between steel bar and concrete was used to identify bond-slip signals in our experiments. The apparatus which could be called “pitch-catch system” consists of a signal generator, a piezoelectric wafer, a resonant AE sensor (PAC R15-ALPHA), and a data acquisition system (here the AE system was employed as the receiver). The piezoelectric wafer was attached to one end of the steel bar, and excited a narrowband 5-cycle Hanning windowed tone burst (five-peaked wave) which was generated by a signal generator. The resonant AE sensor with response frequency of 150 kHz was adhered to the other end of the steel bar to receive the excited ultrasonic signals. This kind of signal can capture the damage information about the interface of steel bar and concrete. From various characteristics of the received signals, such as the time of arrival, amplitude, frequency content, etc., information about the damage can be extracted (Wu and Chang 2006, Raghavan and Cesnik 2007).

The bending load was applied stepwise with 10 kN per step. When the load reached a predetermined level, the displacement was held constant to allow the beam to reach a steady state, and AE signals fade down gradually. Then the “pitch-catch system” is set to monitor the bond-slip state. After this, the specimen was reloaded to the next level. In the entire process, AE signals, which were emitted from damages of cracking, bond-slip, and other kinds of sources including noise, were received by the four AE sensors.

2.2 Pullout tests

Pullout tests were performed to generate bond-slip between steel bar and concrete and analyze the emitting AE signals. The pullout test has been widely used in the investigation of bond behavior. It intuitively manifests the process of bond-slip, and can be used to study AE characteristics of bond-slip. The specimen was designed as a concrete cube with a hot rolled smooth bar cast in the center. A reaction frame was designed to provide reactive force to the concrete cube in the tensile test as shown in Fig. 2. The sectional area of the cube was a square with 100 mm side lengths, and the cube length was 150 mm with 100 mm bond length. An unbounded area was preset at loading side of the cube to reduce the influence of pressure which came from the underplate of the reaction frame. The diameter of the steel bar was 10 mm.

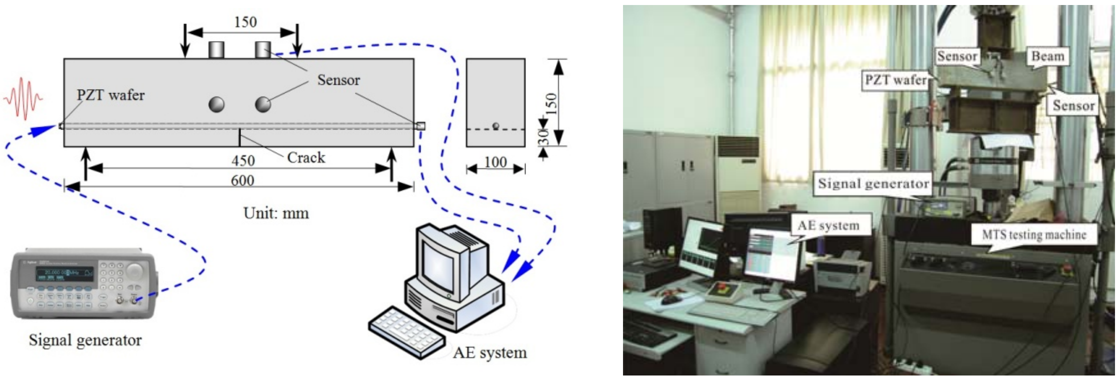

(a) Geometry of specimen (b) experimental setup

Fig. 1 Geometry of specimen and experimental setup

The test was performed on the MTS system. Displacement control was utilized, and the loading velocity was 1 mm/min. At the same time, two AE sensors were adhered to the sides of the cube to collect AE signals.

The loading curve and the AE energy bar graph versus time were shown in Fig. 3. It can be seen from loading curve that the ascending stage was divided into two stages by a turning point which corresponds to the beginning of slip of free end of the steel bar. The loading curves of these two stages showed different linear relationships with time (or with displacement of loading end). The tensile force of the turning point was 10.56 kN. The average bond stress τ_b at this point, which was the tensile force divided by the bond area, was about 3.36 MPa. After the maximum load is reached, the test turned into a residual bonding stage where the load decreased gradually with the loading time.

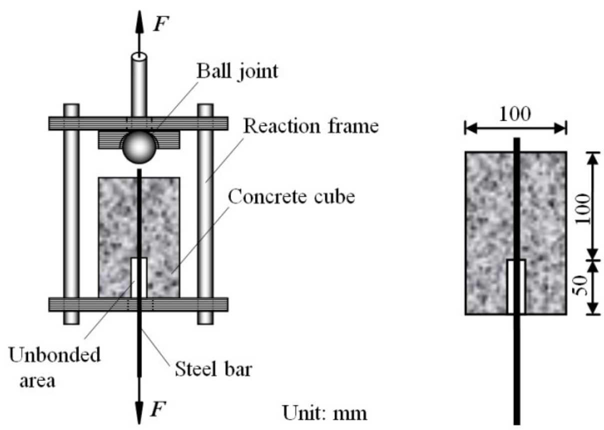

Fig. 2 The setup of pullout test

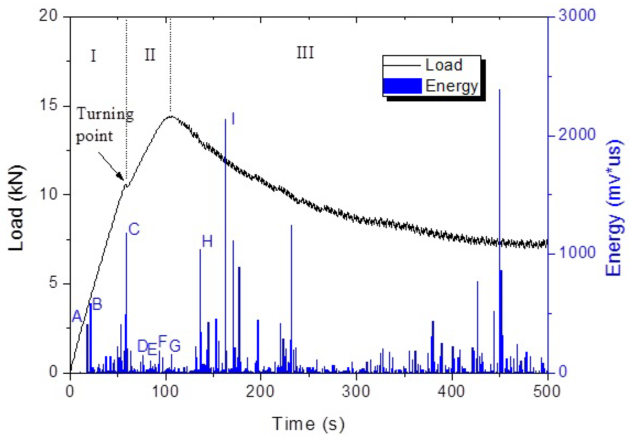

Fig. 3 Loading curve and corresponding AE energy in pullout test

3. Hilbert-Huang transform

The HHT is an empirically based data-analysis method. Its basis of expansion is adaptive so that it can produce physically meaningful representations of data from nonlinear and non-stationary processes (Huang and Shen 2005). The HHT consists of two parts: empirical mode decomposition (EMD) and Hilbert spectral analysis (HSA) (Huang *et al*. 1998). The first step of HHT is to use EMD to sequentially decompose a signal $u(t)$ into n intrinsic mode functions (IMFs) c_i and a residual r_n as

$$u(t) = \sum_{i=1}^{n} c_i + r_n \tag{1}$$

The decomposition is based on the simple assumption that any signal consists of different simple intrinsic modes of oscillations.

Then the Hilbert transform is applied to each IMF component, the following equation is obtained

$$\hat{c}_i(t) = \frac{1}{\pi}\int_{-\infty}^{\infty} \frac{c_i(\tau)}{t-\tau}\mathrm{d}\tau \tag{2}$$

Constructing analytic signal

$$z_i(t) = c_i(t) + j\hat{c}_i(t) = a_i(t)e^{j\phi_i(t)} \tag{3}$$

The amplitude function $a_i(t) = \sqrt{c_i^2(t) + \hat{c}_i^2(t)}$ and the phase function $\phi_i(t) = \arctan\frac{\hat{c}_i(t)}{c_i(t)}$ can be obtained. By computing the instantaneous frequency $\omega_i(t) = \frac{\mathrm{d}\phi_i(t)}{\mathrm{d}(t)}$, the Hilbert spectrum, which shows the time-frequency distribution of the amplitude, is finally obtained

$$H(\omega,t)=\mathrm{Re}\sum_{i=1}^{n}a_i(t)e^{j\int\omega_i(t)\mathrm{d}t} \tag{4}$$

In the process of EMD, if some IMFs show characteristics of noise, which usually display high frequency and undiminished character, it can be eliminated from the original signal. This can be considered a denoising method.

4. Results and discussion

4.1 Analysis of AE signals

In four-point-bending tests, the load-displacement curve and the load-time curve were obtained from the testing machine as shown in the top of Fig. 4. The AE energy bar graph which represents the AE activity was shown at the corresponding displacement and time simultaneously.

The maximum tensile stress for pulling the steel bar out of the concrete beam can be calculated by the bond stress and the bond length. In the pullout test, the average bond stress τ_b was about 3.36 MPa. Based on this stress value, the maximum tensile stress of steel bar for pulling the steel bar out of the concrete beam can be calculated as

$$\sigma_\mathrm{s}=\frac{F_\mathrm{s}}{A_\mathrm{s}}=\frac{\tau_\mathrm{b}\pi d_\mathrm{s}l_\mathrm{s}}{\frac{\pi d_\mathrm{s}^2}{4}}=403.2\ \mathrm{MPa} \tag{5}$$

where, σ_s is the maximum tensile stress of steel bar, F_s the maximum tensile force of bar, A_s and d_s are the sectional area and the diameter of steel bar respectively, τ_b is the average bond stress, and l_s is the bond length. Though the actual value might be lower because the bonding strength would slightly reduce with the increase of bond length, it might still reach or exceed the yielding stress (235 MPa). Thus it is possible for the steel bar to yield in the test. The development of a plastic plateau in the load-displacement curve (Fig. 4) demonstrated the occurrence of yielding. The yielding would lead to significant deformation of steel bar, and accelerate its debonding in concrete. The following dive of loading curve came from the first integral bond slip when one end of the steel bar began to be pulled in.

The parameter "energy" in Fig. 4 reflects the released energy in an AE event. This parameter-based analysis is used to select important signals from a large number of data to perform signal-based analysis. It is notable that the energy is derived from an event rather than a signal. A severe damage event always contains several signals. Due to the wide difference in magnitude of various events, the logarithm of energy named "energy magnitude" was presented as

$$\textit{Energy magnitude}=\log(E) \tag{6}$$

where E is the parameter of "AE energy" received from an AE event. The energy magnitude was similar to the earthquake magnitude in seismology, and was used to initially identify the source. The energy magnitude of some obvious damage events marked "A" to "F" in the loading curve (Fig. 4) were given in Table 1. In contrast, the magnitude of overwhelming majority of AE events was less than 4.0. In pullout test, the maximum magnitude was less than 3.4.

Table 1 Energy magnitude of main damage events

Damage event	A	B	C	D	E	F
Energy magnitude	5.23	5.10	5.31	4.94	4.99	5.02

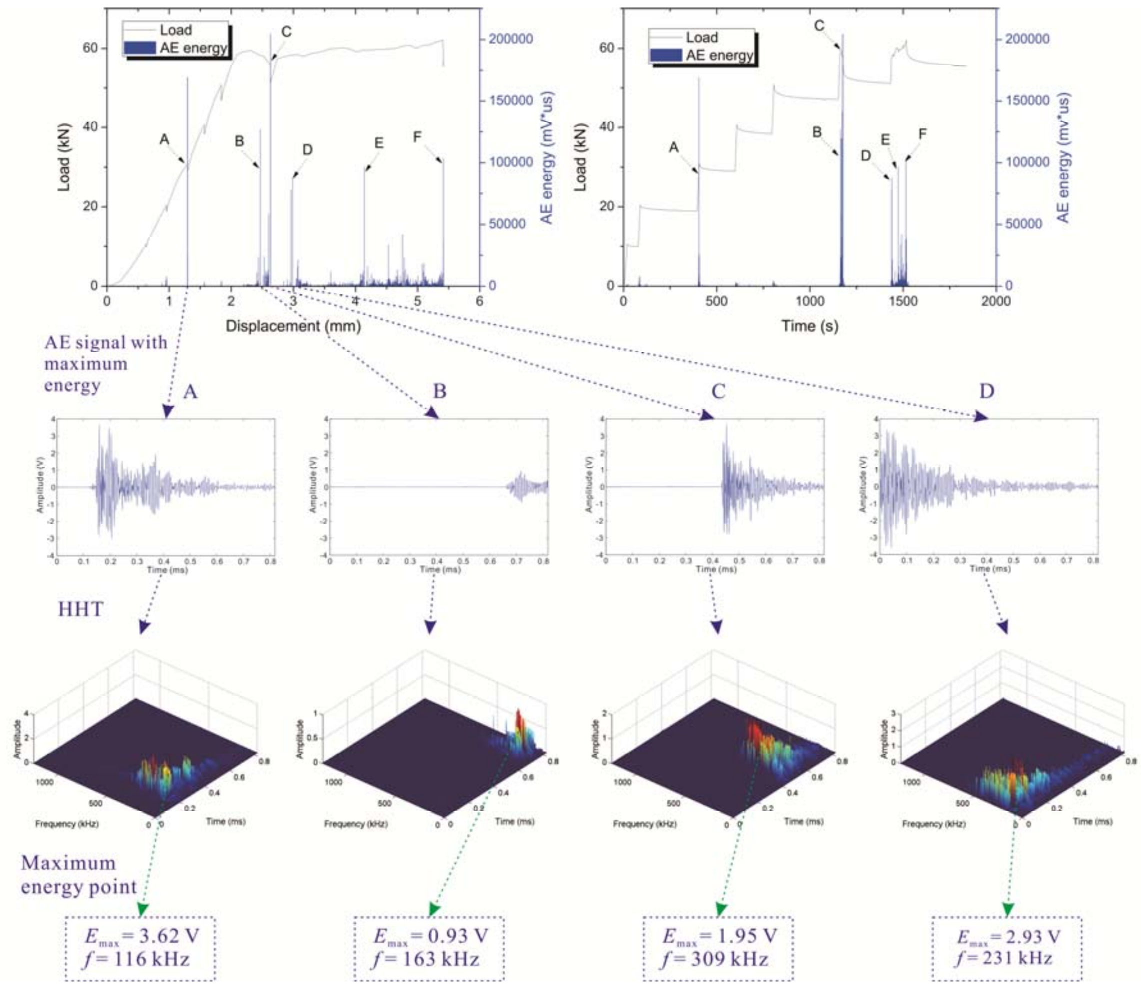

Fig. 4 Analysis procedure to damage events

A severe AE event may contain several AE signals (Fig. 5). One of them with maximum energy reflected the damage state. The others may come from successive activities or edge reflection. The procedure of analysis to a damage event was shown in Fig. 4. The AE signal with maximum energy was chosen from all signals of the event. Using HHT, the corresponding 3D energy spectrum was obtained which could reveal signal features in both time and frequency domains simultaneously. From the time-frequency graph, the maximum energy point could be identified. The corresponding instantaneous energy (named maximum instantaneous energy, MIE, expressed in energy of unit interval, and the units was V·s/s or V) and the instantaneous frequency could be extracted. These characteristics related quantitatively to some damage states, and provided a quantitative analysis in AE technique. This analytical method will be called "MIE method" in the following section.

4.2 Identification of bond-slip in bending test

In the process of identifying the bond-slip signals from other sources, the active pitch-catch method was used. The principle of this method is that the signal amplitude of the sensor increases with the extent of debonding. When bond-slip occurs, the debonding gap between the steel bar and concrete prevents the ultrasonic wave from transmitting outside, consequently more energy be received by the sensor at the end of the steel bar.

Several similar specimens with different debond extents were used experimentally to verify their regularity. It shows that the signal's amplitude of the sensor increases as the extent of debond increases as shown in Fig. 6(a), which was observed by Wu (Wu and Chang 2006) and Wang (Wang *et al*. 2009). It is notable that the amplitude from completely debonding case (corresponding the debonding ratio of 1) was derived by a naked steel bar. This may lead to a higher amplitude than the case that the rebar completely debonding but still embedded in concrete. The steel bar was actively excited by a narrowband five-peaked tone burst wave at 100 kHz, which was demonstrated as a sensitive frequency in concrete studies (Wu and Chang 2006).

In the bending test, the amplitude of five-peaked wave received at the end of the steel bar presents an obvious regular patterns as shown in Fig. 6(b). In the early of the test (before the load of 20 kN), the amplitude keeps almost unchanged. A distinct decrease can be found at the load of 30 kN. We surmise that the decrease caused by the sudden change of interface state after cracking. It can be determined that no bond-slip was emerged before the load of 30 kN. Therefore, the large energy event emerged at about 30 kN and marked "A" in Fig. 4 came from a "pure" cracking damage (Fig. 7(a)). It is worth noting that the data point corresponding to a certain load in Fig. 6 (b) was recorded at the end of the holding stage of that load.

The increase of amplitude after 30 kN (Fig. 6(b)) showed that the bond-slip damage began in the loading period from 30 kN to 40 kN. According to the variation of amplitude and its change law with debonding in Fig. 6(a), the debonding length in this period was very limited. Thus did the next loading period (from 40 kN to 50 kN). However, a significant increase of the amplitude which indicated a severe bond slip occurred after the load step of 60 kN. A conspicuous dive in loading curve (point C in Fig. 4) verified this bond slip.

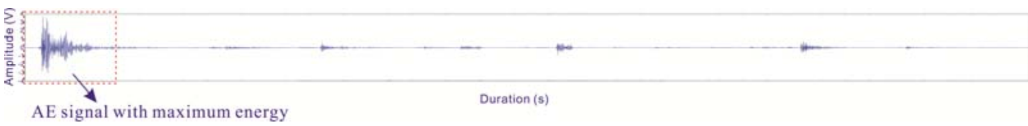

Fig. 5 A severe damage event (event A) which contains several AE signals

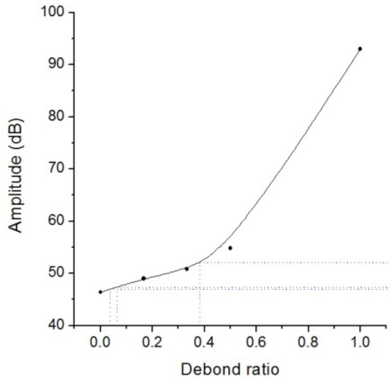

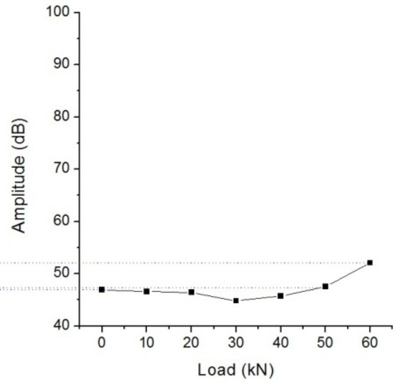

(a) Result of static test (b) Result of bending test

Fig. 6 Variation of wave amplitude received on the steel bar with debond ratio and loading process in bending test

(a) 80 mm initial cracking

(b) The steel bar pulled in

(c) Cracking state after failure

Fig. 7 Visible damages of the beam

In addition, the AE characteristics of bond slip which were derived in pullout tests can be used to identify the bond slip in bending test. Some typical AE signals of pullout tests marked "A" to "I" in Fig. 3 were analyzed by using the "MIE method". Their frequency characteristics were extracted and listed in table 2. It shows that the frequency of bond slip signals is in the range of 222 to 347 kHz, and a severe slipping event always emits signals with higher frequency. By comparing the signal of event C in bending test with these frequency characteristics, it can be seen that the frequency of 309 kHz indicates a typical slipping feature.

Table 2 Frequency characteristics of bond slip signals in pullout test

Damage event	A	B	C	D	E	F	G	H	I
Frequency (kHz)	325	271	347	222	275	297	319	319	319

Table 3 AE characteristics of severe damages in concrete members

Damage	Event	MIE (V·s/s)	Frequency (kHz)	Summary
Cracking (80 mm)	A	3.62	116	The MIE is related to the sudden instantaneous occurrence of a damage event. One signal from initial cracking released the largest energy. In the "failure" process, different damage events show different frequency feature which has a rising tendency with the evolution of destruction.
Steel yielding	B	0.93	163	
Bond slip	C	1.95	309	
Mixed damage	D	2.93	231	In later stage, the damage dominated by bond slip. The last collapse shows cracking feature.
	E	1.75	381	
	F	0.32	126	

4.3 Discussion

With the loading curve and the damage inspection using active pitch-catch technique, the damage states associated with AE signals can be identified. The mechanisms of the severe damage events indicated in Fig. 4 can also be summarized as follow. The first event A arose from the coalescence of a macro cracking which indicated the end of the uncracked stage. Then the beam entered into the second stage, i.e., cracking stage. The crack expanded and tensile stress of reinforcement increased with loading, untill the steel bar began to yield. The event B arose from the beginning of yielding which indicated the beginning of failure stage. The event C is mainly associated with a severe bond-slip damage corresponding to the beginning of slip of one end of the steel bar. Although this process was accompanied by the cracking of concrete (the crack propagation was visible), the signal feature of strong slipping overrode that of weak cracking. Both the analysis of pitch-catch signals and the comparison of AE characteristics confirmed its slipping feature. After the occurrence of integral bond slip, the yielding of steel bar will no longer appear. In this period, the existence of reinforcement made the damage evolve gradually. The damages mainly came from cracking and bond slippage, and the latter dominated the damage process in this period. One end of the steel bar which overhung at the beginning was pulled into the concrete (Fig. 7(b)).

By the quantitative method, the MIE and the corresponding frequency which reflected source mechanisms were determined. The event A came from a "pure" cracking. A fracture occurs when the energy available for crack growth is sufficient to overcome the resistance of the material. Therefore, once a macro cracking began, enormous energy would drive a considerable cracking. It is notable that the preset notch of the beam is not a real sharp crack, and the initial cracking shall need more energy. The crack length in event A reached 80 mm, and MIE reached 3.62 V·s/s. The corresponding frequency was 116 kHz which indicated a low frequency in concrete cracking. Event B is dominated by the yielding of steel bar, which showed higher frequency. In this period, the stress of steel bar remained unchanged, and the crack of the concrete further developed. Event C which caused the decrease of load arose from a severe bond slip. The MIE was higher than that of B, and the corresponding frequency reached 309 kHz which was relatively a high frequency. Later, the change of depth of compression zone made the load slightly increase. Event D to F occurred in this period might originate from cracking, slipping, or their combination. From analysis of frequency feature, event D and E came from bond slip, and event F corresponding to the collapse of the beam mainly came from cracking of concrete (Fig. 7(c)). The characteristics of these special signals were concluded in Table 3.

The integral bond slip which was presented as event C in AE measurement can be regarded as the sign of “failure”. The destruction of the RC beam underwent three processes before the “failure”: cracking of concrete, yielding of rebar, and bond slip. The signal characteristics in energy and frequency possess a certain regular pattern in these processes, which were also summarized in Table. 3. It was noted that the attenuation in wave propagation which was serious for high frequency might influence the result. But for signals received at short range, the influence could be ignored.

5. Conclusions

AE characteristics of RC members were investigated experimentally to identify the AE source mechanism of damage evolution. Bending tests of the RC beam was designed to show some typical damages. With loading curve and damage inspection using an active pitch-catch technique, the damage states associated with AE signals were identified. A pullout test was also performed to understand the inherent AE characteristics of bond-slip. The maximum instantaneous energy and the corresponding instantaneous frequency of typical signals were presented to provide a quantitative assessment to the RC beam using AE technique. The HHT was used to help extracting signal characteristics.

Based on the energy magnitude, some important damage events with large energy release in the experiment were analyzed, and three damage stages were distinguished. The maximum instantaneous energy and the corresponding frequency were derived by using a quantitative method (MIE method). Their characteristics followed a specific pattern in failure process which can be used to quantify the damage severity of concrete components. Both the cracking signal with maximum MIE, and the bond slip signal with maximum frequency can be used as warning signs for different degrees of destruction in loading capacity. In later stage (after the failure point), the beam still retained some bearing capacity. The damages were dominated by bond slip until the beam collapse which was mainly caused by cracking of the concrete.

Acknowledgements

The authors are grateful to the Natural Science Foundation of China (No. 11272138) and (No. 11172114) for supporting this work.

References

Aggelis, D.G., Mpalaskas, A.C. and Matikas, T.E. (2013), “Investigation of different fracture modes in cement-based materials by acoustic emission”, *Cement Concrete Res.*, **48**, 1-8.

Aldahdooh, M.A.A. and Bunnori, N.M. (2013), “Crack classification in reinforced concrete beams with varying thicknesses by mean of acoustic emission signal features”, *Constr. Build. Mater.*, **45**, 282-288.

Balázs, G., Grosse, C., Koch, R. and Reinhardt, H. (1993), “Acoustic emission monitoring on steel-concrete interaction”, *Otto Graf J.*, **4**, 56-90.

Beattie, A.G. (1983), "Acoustic emission, principles and instrumentation", *J. Acoust. Emission*, **2**(1-2), 95-128.

Enoki, M. and Kishi, T. (1988), "Theory and analysis of deformation moment tensor due to microcracking", *Int. J. Fracture*, **38**(4), 295-310.

Frank Pai, P. and Palazotto, A.N. (2008), "HHT-based nonlinear signal processing method for parametric and non-parametric identification of dynamical systems", *Int. J. Mech. Sci*., **50**(12), 1619-1635.

Govekar, E., Gradišek, J. and Grabec, I. (2000), "Analysis of acoustic emission signals and monitoring of machining processes", *Ultrasonics*, **38**(1-8), 598-603.

Grosse, C.U. and Finck, F. (2006), "Quantitative evaluation of fracture processes in concrete using signal-based acoustic emission techniques", *Cement Concrete Comp*., **28**(4), 330-336.

Grosse, C. U. and L. M. Linzer (2008). Signal-Based AE Analysis. Berlin Germany, Springer.

Hamdi, S.E., Le Duff, A., Simon, L., Plantier, G., Sourice, A. and Feuilloy, M. (2013), "Acoustic emission pattern recognition approach based on Hilbert-Huang transform for structural health monitoring in polymer-composite materials", *Appl. Acoust.*, **74**(5), 746-757.

Han, W.Q. and Zhou, J.Y. (2013), "Acoustic emission characterization methods of damage modes identification on carbon fiber twill weave laminate", *Sci. China-Technol. Sci*., **56**(9), 2228-2237.

Huang, N.E. and Shen, S.S.P. (2005), *Hilbert-Huang Transform and its application. Singapore*, World Scientific Publishing Co. Pte. Ltd.

Huang, N.E., Shen, Z., Long, S.R., Wu, M.C., Shih, H.H., Zheng, Q., Yen, N.C., Tung, C.C. and Liu, H.H. (1998), "The empirical mode decomposition and the Hilbert spectrum for nonlinear and non-stationary time series analysis", *P. Roy. Soc. A. Math. Phys*., **454**(1971), 903-995.

Law, L.S., Kim, J.H., Liew, W.Y.H. and Lee, S.K. (2012), "An approach based on wavelet packet decomposition and Hilbert-Huang transform (WPD-HHT) for spindle bearings condition monitoring", *Mech. Syst. Signal Pr*., **33**, 197-211.

Lin, L. and Chu, F. (2011), "Feature extraction of AE characteristics in offshore structure model using Hilbert–Huang transform", *Measurement*, **44**(1), 46-54.

Lin, L. and Chu, F. (2012), "HHT-based AE characteristics of natural fatigue cracks in rotating shafts", *Mech. Syst. Signal Pr*., **26**, 181-189.

Lu, C., Ding, P. and Chen, Z. (2011), "Time-frequency analysis of acoustic emission signals generated by tension damage in CFRP", *Procedia Eng*., **23**, 210-215.

Ohtsu, M., Shigeishi, M. and Sakata, Y. (1998), "Nondestructive evaluation of defects in concrete by quantitative acoustic emission and ultrasonics", *Ultrasonics*, **36**(1-5), 187-195.

Ono, K. (1994), "Trends of recent acoustic emission literature", *J. Acoust. Emission*, **12**, 177-198.

Raghavan, A. and Cesnik, C.E. (2007), "Review of guided-wave structural health monitoring", *Shock Vib. Digest*, **39**(2), 91-116.

Sachse, W. and Kim, K.Y. (1987), "Quantitative acoustic emission and failure mechanics of composite materials", *Ultrasonics*, **25**(4), 195-203.

Sagar, R.V. and Prasad, B.K.R. (2012), "A review of recent developments in parametric based acoustic emission techniques applied to concrete structures", *J. Nondestruct. Eval*., **27**(1), 47-68.

Wang, Y., Zhu, X., Hao, H. and Ou, J. (2009), "Guided wave propagation and spectral element method for debonding damage assessment in RC structures", *J. Sound Vib*., **324**(3-5), 751-772.

Wu, F. and Chang, F.K. (2006), "Debond detection using embedded piezoelectric elements for reinforced concrete structures - Part II: analysis and algorithm", *Struct. Health Monit*., 5(1), 17-28.

Yoon, D., Weiss, W. and Shah, S. (2000), "Assessing damage in corroded reinforced concrete using acoustic emission", *J. Eng. Mech. – ASCE*, **126**(3), 273-283.

Yuyama, S., Okamoto, T., Shigeishi, M. and Ohtsu, M. (1995), "Quantitative evaluation and visualization of cracking process in reinforced concrete by a moment tensor analysis of acoustic emission", *Mater. Eval*., **53**(6), 751-756.

BS